Thermodynamics of polymer/diluent systems for thermally induced phase separation: 2. Solid–liquid phase separation systems

Sung Soo Kim and Douglas R. Lloyd*
Department of Chemical Engineering, Centre for Polymer Research, The University of Texas at Austin, Austin, TX 78712, USA
(Received 7 January 1991; accepted 30 March 1991)

Thermodynamic analysis of solid–liquid phase separation was performed using Flory's equation of state theory adapted to polymer/oligomer systems. Interaction parameters were estimated for isotactic polypropylene/n-alkane and isotactic polypropylene/n-fatty acid systems using parameters determined in the previous paper in this series. The adapted Flory's equation of state theory and parameters proved reliable by comparing the estimated interaction parameters with the experimental ones obtained from melting temperature depression measurements. Isotactic polypropylene/n-alkane systems have dominant free volume effects. Isotactic polypropylene/n-fatty acid systems have greater enthalpic interactions than isotactic polypropylene/n-alkane systems due to the functional end group of the n-fatty acid. The free volume effect decreased with increasing chain length. Isotactic polypropylene/n-alkane systems were stable within the temperature range of interest, and isotactic polypropylene/n-fatty acid systems were expected to be unstable at temperatures below the iPP crystallization curves.

(Keywords: interaction parameter; phase separation; equation of state)

INTRODUCTION

In the previous paper in this series[1] and other publications[2–10], it was mentioned that thermodynamic study of polymer/diluent systems is important in interpreting the thermally induced phase separation (TIPS) mechanism and the resulting structure in TIPS membrane formation. In this paper thermodynamic analysis was performed for model systems undergoing solid–liquid phase separation via polymer crystallization. The analysis uses Flory's equation of state (EOS) theory adapted to the polymer/oligomer systems, as introduced in reference 1. Several isotactic polypropylene (iPP)/n-alkane and iPP/n-fatty acid systems were selected for this study.

The objective of this paper was to evaluate the adapted Flory's EOS theory[1,11–13] for its ability to represent accurately the polymer/diluent phase behaviour for the model systems listed above. The influences of diluent chain length and functional groups on the polymer/diluent interaction and phase behaviour were investigated in this paper. Since TIPS membrane structure has been shown to vary with melt blend composition and thermal history, another objective was to determine the variation of the appropriate interaction parameters with temperature and composition in these model systems. Ultimately, the knowledge gained from this study will enable one to predict phase boundary and solution stability in polymer/diluent systems capable of producing microporous structures via TIPS.

The EOS parameters for the model systems were determined in the previous paper[1], and were used in this paper to estimate the thermodynamic properties by Flory's EOS. The estimated polymer/diluent interaction parameters were compared with those from melting temperature depression measurement to confirm the validity of the estimation as well as the EOS parameter determination in reference 1.

INTERACTION PARAMETER ESTIMATION BY EOS THEORY

Flory's EOS theory was adapted by the polymer/oligomer system in the previous paper in this series[1]. The residual chemical potential of the diluent or polymer was derived from the adapted Flory's EOS theory.

$$\Delta\mu_i^R/RT = \chi_{\mu i} r_i \phi_j^2 \quad (1)$$

$$= (\bar{H}_i^R - T\bar{S}_i^R)/RT \quad (2)$$

where r_i is the number of segments of i component molecule, ϕ_j is the volume fraction of j component, and $\bar{H}_i^R$ and $\bar{S}_i^R$ are the partial molar residual enthalpy and entropy, respectively, as introduced in equations (5) and (6) in reference 1. According to Sanchez's classification of composition-dependence interaction parameters, χ in the $\Delta G/RT$ equation (equation (1) in reference 1) must be changed to $\chi_{\mu i}$ in the $\Delta\mu_i^R/RT$ equation (equation (1) above)[14].

The interaction parameter ($\chi_{\mu i}$) can be divided into enthalpic ($\chi_{\mu ih}$) and entropic ($\chi_{\mu is}$) contributions

$$\chi_{\mu i} = \chi_{\mu is} + \chi_{\mu ih} \quad (3)$$

Each contribution is derived from the partial molar residual entropy and enthalpy as

* To whom correspondence should be addressed
0032-3861/92/051036-11

$$\chi_{\mu is} = -T\bar{S}_i^R/(RTr_i\phi_j^2) \quad (4)$$

$$\chi_{\mu ih} = \bar{H}_i^R/(RTr_i\phi_j^2) \quad (5)$$

where $\chi_{\mu ih}$ is from the enthalpic interaction between polymer and diluent, which usually decreases with increasing temperature for the repulsive interacting system, and $\chi_{\mu is}$ is from the free volume effect, which increases with increasing temperature for any system[12,15]. $\chi_{\mu 1}$ and $\chi_{\mu 2}$ were obtained as the sum of these two contributions.

$$\chi_{\mu 1} = (P_1^*V_1^*/RTr_1\phi_2^2)\{3\tilde{T}_1 \ln[(\tilde{V}_1^{1/3} - 1)/(\tilde{V}^{1/3} - 1)] + (\tilde{V}_1^{-1} - \tilde{V}^{-1})\} + (V_1^*/RTr_1\phi_2^2)(\theta_2^2X_{12}/\tilde{V}) \quad (6)$$

$$\chi_{\mu 2} = (P_2^*V_2^*/RTr_2\phi_1^2)\{3\tilde{T}_2 \ln[(\tilde{V}_2^{1/3} - 1)/(\tilde{V}^{1/3} - 1)] + (\tilde{V}_2^{-1} - \tilde{V}^{-1})\} + (V_2^*/RTr_2\phi_2^2)(\theta_2^2X_{12}/\tilde{V}) \quad (7)$$

In this paper the interaction parameters ($\chi_{\mu 1}$ and $\chi_{\mu 2}$) for iPP/n-alkanes and iPP/n-fatty acids systems in the temperature range of interest were estimated by equations (6) and (7) and compared with $\chi_{\mu 2}$ determined by melting temperature (T_m) depression measurement. An entropic contribution due to the specific interaction (Q_{12}) was ignored for the systems in this study as suggested by Chahal *et al.*[16] and Sham and Walsh[17], since iPP and the diluents are relatively non-polar.

INTERACTION PARAMETER FROM MELTING TEMPERATURE DEPRESSION

The chemical potential of the polymer per repeat unit is derived by differentiating the $\Delta G/RT$ equation (equation (1) in reference 1) with respect to moles of polymer molecules (n_2)[18].

$$\mu_u^{sol} - \mu_u^0 = RT[1/r_2 \ln \phi_2 - (1/r_1 - 1/r_2)\phi_1 + \chi_{\mu 2}\phi_1^2] \quad (8)$$

where μ_u^{sol} is the chemical potential of polymer units in the solution phase and μ_u^0 is that of pure polymer melt at the same temperature.

The chemical potential of crystal (μ_u^c) per repeat unit is defined as

$$\mu_u^c - \mu_u^0 = -\Delta H_{fu}(1 - T/T_m^0) \quad (9)$$

where μ_u^c is the chemical potential of the pure polymer crystal unit at temperature T, ΔH_{fu} is the enthalpy change of melting a polymer single crystal unit, and T_m^0 is the equilibrium melting temperature of pure polymer. At the equilibrium melting temperature of polymer in the presence of diluent, μ_u^c equals μ_u^{sol}.

The combination of equations (8) and (9) makes the T_m depression equation

$$[(1/r_1 - 1/r_2)\phi_1 - 1/r_2 \ln \phi_2] - (1/T_m - 1/T_m^0)(\Delta H_{fu}/R) = \chi_{\mu 2}\phi_1^2 \quad (10)$$

where T_m and T_m^0 are the equilibrium melting temperature of the polymer in a mixture and in the pure state, respectively[18,19].

Melting temperature depression measurement

iPP of weight average molecular weight 243 000 and degree of polymerization 1033 was supplied by Himont Co. (Profax 6723, lot no. 79316). In the literature T_m^0 of iPP is given as 460.5 K and ΔH_{fu} is given as 6930 J mol^{-1} of repeat unit for iPP[20]. These values were confirmed by experimental results (T_m^0 = 460.5 K, ΔH_{fu} = 6955 J mol^{-1} per repeat unit of iPP). n-Alkanes ($C_{14}H_{30}$, $C_{20}H_{42}$, $C_{32}H_{66}$) were purchased from Alfa Products, and n-fatty acids ($C_{14}H_{29}COOH$, $C_{19}H_{39}COOH$) were obtained from Aldrich Chemical Co.

Homogeneous polymer/diluent mixtures were prepared in test tubes in a hot oven. To prevent oxidation during mixing, the test tube was purged with N_2 and sealed before heating in the hot oven. Each sample composition was confirmed by measuring the amount of diluent removed using a Soxhlet apparatus. A Perkin–Elmer DSC 7 was used to measure the melting temperature of each sample. Initially the sample was heated to 473 K and held there for 10 min to minimize any thermal history. It was reported by Lim that the initial holding at 473 K for 10 min was sufficient to minimize the thermal history[21]. The sample was then quenched to the desired crystallization temperature (T_c) and held there for a specified crystallization time before heating. The heating rate was 10 K min^{-1} and the endotherm peak temperature was taken as the melting temperature.

Equilibrium melting temperatures were determined using a Hoffman–Weeks plot[22]; a typical plot is shown in *Figure 1*. The other Hoffman–Weeks plots are given in reference 23. Equilibrium T_m depression curves for n-alkane and n-fatty acid systems are plotted in *Figure 2*. With a decrease in the number of carbons in the diluent, T_m is further depressed for both n-alkanes and n-fatty acids. Depression by n-fatty acid is less than that by n-alkane with the similar number of carbons, since the acids have a greater interaction parameter than n-alkanes due to the functional group at the end of the chain (–COOH).

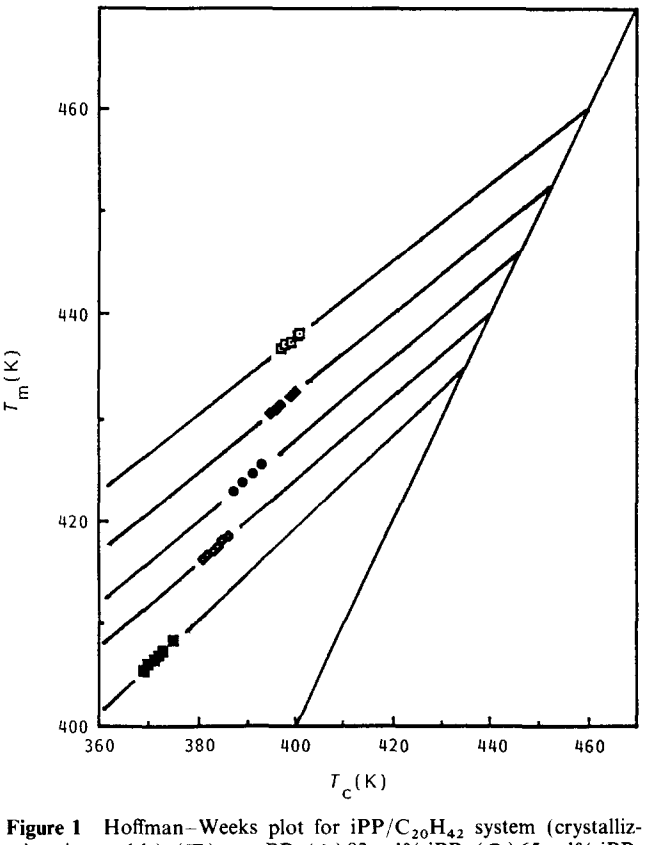

Figure 1 Hoffman–Weeks plot for iPP/$C_{20}H_{42}$ system (crystallization time = 1 h): (□) pure PP; (◆) 83 vol% iPP; (●) 65 vol% iPP; (◇) 47 vol% iPP; (■) 18 vol% iPP

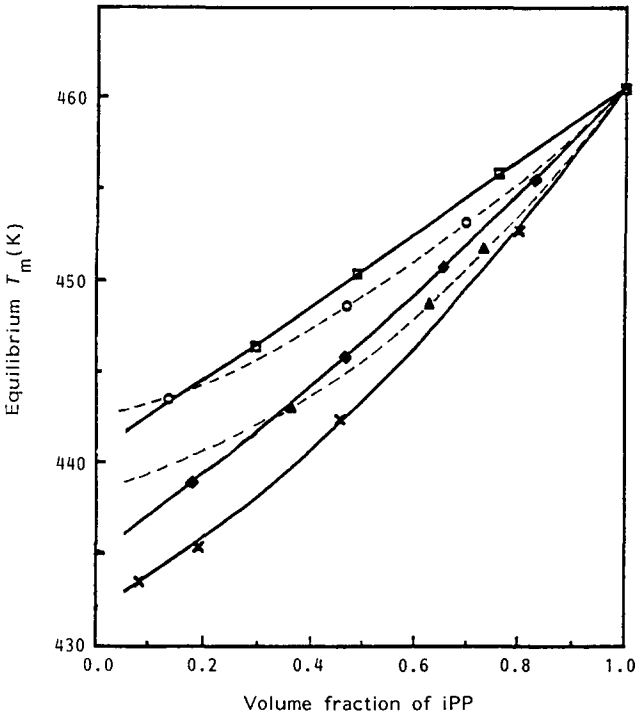

Figure 2 Equilibrium melting temperatures of iPP/n-alkane and iPP/n-fatty acid systems: (□) iPP/$C_{32}H_{66}$; (◆) iPP/$C_{20}H_{42}$; (×) iPP/$C_{14}H_{30}$; (○) iPP/$C_{19}H_{39}COOH$; (▲) iPP/$C_{14}H_{29}COOH$

Interaction parameter determination from melting temperature depression

Based on equation (10), a linear plot of

$$[(1/r_1 - 1/r_2)\phi_1 - 1/r_2 \ln \phi_2] - (1/T_m - 1/T_m^0)(\Delta H_{fu}/R)$$

versus ϕ_1^2 was obtained. $\chi_{\mu 2}$ at T_m can be determined from the slope of the plot, and ΔH_{fu} can be determined from the intercept of the plot. It must be noted that $\chi_{\mu 2}$ obtained by this procedure is not a value at a specific composition and corresponding T_m. That is, the procedure is based on the assumption that $\chi_{\mu 2}$ is independent of composition and temperature within the T_m depression range of each mixture. Therefore, it is reasonable to regard these $\chi_{\mu 2}$ values as those at the iPP volume fraction of 0.5 and corresponding T_m for each mixture.

$$[(1/r_1 - 1/r_2)\phi_1 - 1/r_2 \ln \phi_2] - (1/T_m - 1/T_m^0)(\Delta H_{fu}/R)$$

is plotted *versus* ϕ_1^2 for iPP/n-alkanes and iPP/n-fatty acids in *Figure 3*. In every case a linear plot was obtained with $R^2 = 0.95$–1.00, the slope of which is $\chi_{\mu 2}$ as indicated by equation (10).

With an increase in the number of carbons in the diluent, $\chi_{\mu 2}$ decreases for both n-alkane and n-fatty acid systems. As the chain length of the diluent increases, the diluent approaches the polymeric structure and the free volume effect decreases, thereby causing $\chi_{\mu 2}$ to decrease. In terms of enthalpic interactions, as the chain length of n-fatty acid increases, the density of carboxyl group decreases and so does the interaction parameter, which was reflected in reference 1 as a decrease in X_{12}. Moreover, increasing the chain length reduces the chain end effect and leads to a decrease in the interaction parameter.

$\chi_{\mu 2}$ of an iPP/n-fatty acid system is greater than that of an iPP/n-alkane of similar chain length. That is, $\chi_{\mu 2}$s of iPP/$C_{14}H_{29}COOH$ and iPP/$C_{19}H_{39}COOH$ systems are greater than those of iPP/$C_{14}H_{30}$ and iPP/$C_{20}H_{42}$ systems, respectively. The enthalpic interaction between iPP and n-fatty acid is much greater than that between iPP and n-alkane due to the carboxyl group at the end of the n-fatty acid.

COMPARISON OF ESTIMATED AND EXPERIMENTAL INTERACTION PARAMETERS

$\chi_{\mu 2}$ was estimated at an iPP volume fraction of 0.5 and compared with that from the T_m depression method for each system in *Figures 4* and *5*. For iPP/n-alkane systems they were in good agreement with the maximum deviation being 3×10^{-3} for the iPP/$C_{14}H_{30}$ system. The deviation decreased with increasing chain length. iPP/n-fatty acid systems also have fairly good agreement between experimental and estimated $\chi_{\mu 2}$ with a slight underestimation. This deviation might result from the determination of X_{12} parameters by extrapolation in Figure 9 in reference 1. For both iPP/n-alkane and iPP/n-fatty acid systems, increased chain length of diluent within the same class of diluent decreased the interaction parameter.

The critical composition (ϕ_{2c}) and the critical interaction parameter ($\chi_{\mu 2c}$) of the system are important for the system stability test and for predicting an upper critical solution temperature (*UCST*) and a lower critical solution temperature (*LCST*). If $\chi_{\mu 2}$, at a certain temperature and ϕ_{2c}, is greater than $\chi_{\mu 2c}$, the system is unstable. A *UCST* or an *LCST* is the point where $\chi_{\mu 2}$ becomes identical to $\chi_{\mu 2c}$ at ϕ_{2c}. ϕ_{2c} and $\chi_{\mu 2c}$ can be obtained by applying the critical point conditions with

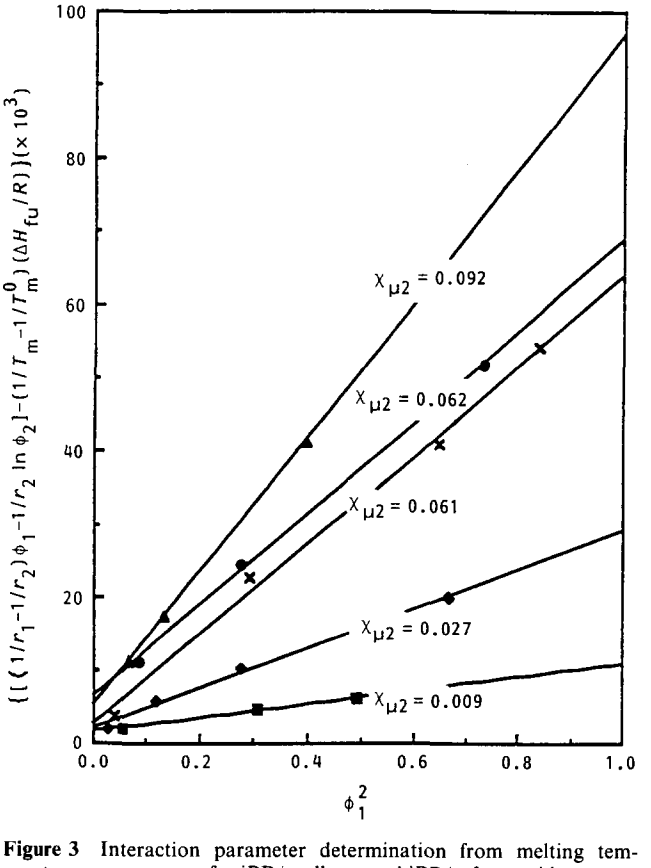

Figure 3 Interaction parameter determination from melting temperature measurement for iPP/n-alkane and iPP/n-fatty acid systems: (▲) iPP/$C_{14}H_{29}COOH$; (●) iPP/$C_{19}H_{39}COOH$; (×) iPP/$C_{14}H_{30}$; (◆) iPP/$C_{20}H_{42}$; (■) iPP/$C_{32}H_{66}$

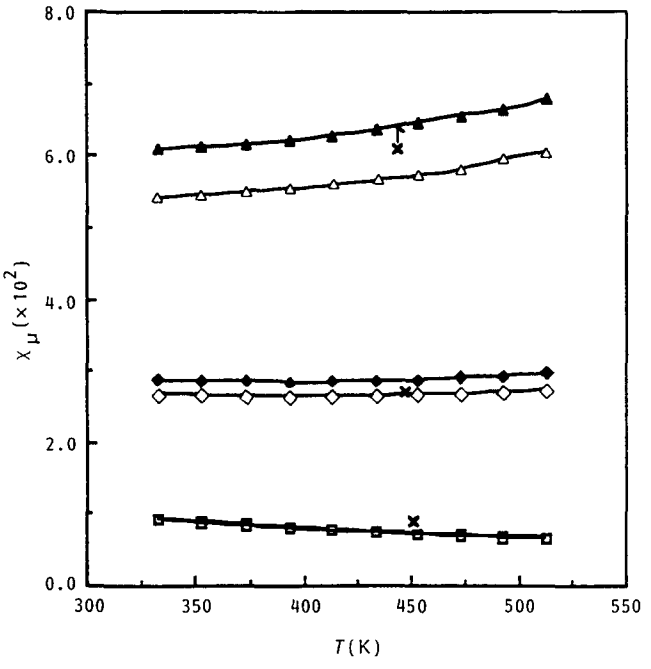

Figure 4 Temperature dependence of interaction parameter for iPP/n-alkane systems at iPP volume fraction = 0.5 (open symbols: $\chi_{\mu 1}$; closed symbols: $\chi_{\mu 2}$): (△, ▲) iPP/$C_{14}H_{30}$; (◇, ◆) iPP/$C_{20}H_{42}$; (□, ■) iPP/$C_{32}H_{66}$; (×) $\chi_{\mu 2}$ from T_m depression

the assumption of a composition independent interaction parameter[15,18].

$$\partial(\Delta\mu_2^R/RT)/\partial\phi_2 = 1/(r_2\phi_2) - (1/r_2 - 1/r_1) - 2\chi_{\mu 2}(1-\phi_2) = 0 \quad (11)$$

$$\partial^2(\Delta\mu_2^R/RT)/\partial\phi_2^2 = -1/(r_2\phi_2^2) + 2\chi_{\mu 2} = 0 \quad (12)$$

$$\phi_{2c} = 1/[1 + (r_2/r_1)^{1/2}] \quad (13)$$

$$\chi_{\mu 2c} = (1/2)(1/r_2^{1/2} + 1/r_1^{1/2})^2 \quad (14)$$

The $\chi_{\mu 2c}$ value for each system was estimated by using $r^2 = 1033$ (degree of polymerization of iPP) and each estimated r_1 value at 450 K as listed in *Table 1*.

The $\chi_{\mu 2c}$ value of a polymer/oligomeric diluent system decreases with increasing chain length of diluent (r_1). For a polymer/simple solvent system, $r_1 = 1.0$ and $\chi_{\mu 2c} = 0.5$ as proposed by Flory[19]. The $\chi_{\mu 2}$ parameter without consideration of $\chi_{\mu 2c}$ or r_1 and r_2 of the system is not a proper parameter representing the system miscibility, and the $\chi_{\mu 2}$ parameters based on different $\chi_{\mu 2c}$s are not directly comparable with each other. The ratio of $\chi_{\mu 2}$ to $\chi_{\mu 2c}$ is a reasonable parameter for comparing systems, and is listed in *Table 1* at each equilibrium melting temperature. In this study, the molecular weight distribution effect was ignored for both iPP and diluents.

Contributions of enthalpic and entropic interaction parameters

$\chi_{\mu 2s}$ and $\chi_{\mu 2h}$ were estimated separately by equations (4) and (5), and $\chi_{\mu 2}$ was obtained by summing these two contributions. The interaction parameter variations with temperature at the critical compositions are shown in *Figures 6–8* for iPP/n-alkane systems and in *Figures 9* and *10* for iPP/n-fatty acid systems. With increasing temperature $\chi_{\mu 2h}$ decreased due to the decrease in enthalpic interaction, and $\chi_{\mu 2s}$ increased due to the increase in free volume effect.

For iPP/n-alkane systems covered in this study, the $\chi_{\mu 2s}$ contribution to $\chi_{\mu 2}$ was significant, since the free volume effect was usually great in the polymer/diluent system. The $\chi_{\mu 2h}$ contribution to $\chi_{\mu 2}$ was small, since the iPP/n-alkane system was non-polar/non-polar and had a small enthalpic interaction. It was proved that the Flory–Huggins theory could not accurately estimate the interaction parameters for these systems, which have a significant free volume effect. Therefore, the advantage of EOS theory over Flory–Huggins theory for the estimation of polymer/diluent system was illustrated.

With the increase of the chain length of n-alkane the free volume effect ($\chi_{\mu 2s}$) decreased, since the difference in EOS parameters decreased. This trend was also true for $\chi_{\mu 2}$, since $\chi_{\mu 2}$ mainly depends on $\chi_{\mu 2s}$ for iPP/n-alkane systems. Therefore, the miscibility of the iPP/n-alkane system was enhanced with the increase in chain length of n-alkane, mainly due to the decrease of free volume effect. The ratio of $\chi_{\mu 2}/\chi_{\mu 2c}$ of iPP/$C_{32}H_{66}$ was the smallest (most miscible) and that of iPP/$C_{14}H_{30}$ was the greatest (least miscible) as listed in *Table 1*.

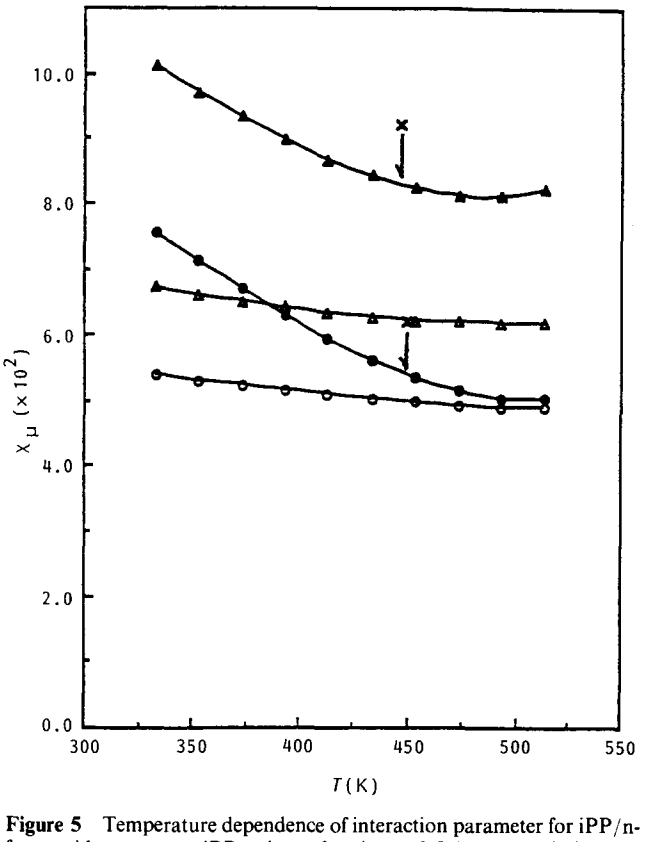

Figure 5 Temperature dependence of interaction parameter for iPP/n-fatty acid systems at iPP volume fraction = 0.5 (open symbols: $\chi_{\mu 1}$; closed symbols: $\chi_{\mu 2}$): (△, ▲) iPP/$C_{14}H_{29}COOH$; (○, ●) iPP/$C_{19}H_{39}COOH$; (×) $\chi_{\mu 2}$ from T_m depression

Table 1 Critical compositions and critical interaction parameters of iPP/n-alkane and iPP/n-fatty acid systems

System	Temperature (K)	r_1	ϕ_{2c}	$\chi_{\mu 2c}$	$\chi_{\mu 2}/\chi_{\mu 2c}$
iPP/$C_{14}H_{30}$	444.1	5.84	0.070	0.099	0.616
iPP/$C_{20}H_{42}$	447.6	7.74	0.080	0.076	0.355
iPP/$C_{32}H_{66}$	451.0	11.56	0.096	0.053	0.170
iPP/$C_{14}H_{29}COOH$	446.8	5.80	0.070	0.100	0.920
iPP/$C_{19}H_{39}COOH$	449.6	7.47	0.078	0.079	0.785

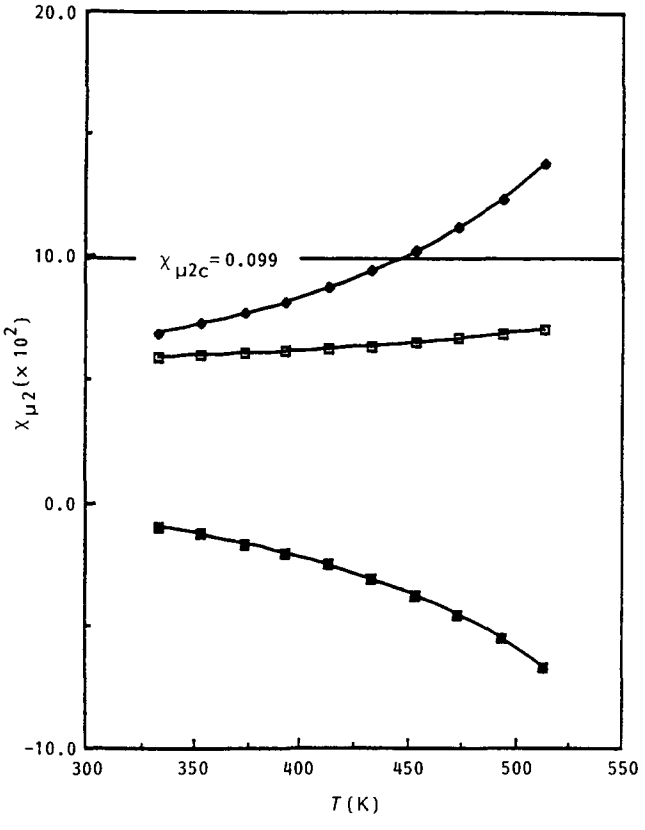

Figure 6 Contributions of enthalpic and entropic interaction parameters for iPP/$C_{14}H_{30}$ system at its critical composition: (□) $\chi_{\mu 2}$; (◆) $\chi_{\mu 2s}$; (■) $\chi_{\mu 2h}$

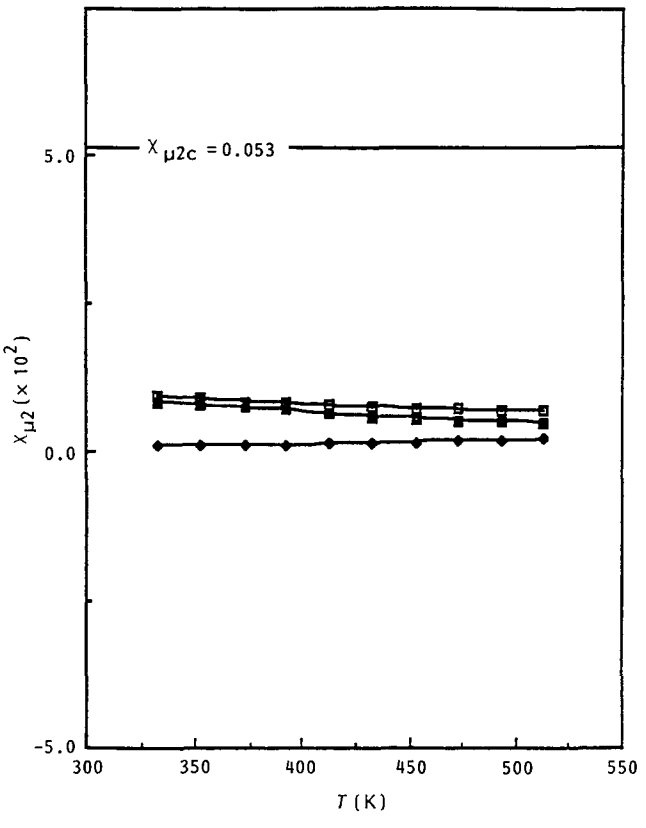

Figure 8 Contributions of enthalpic and entropic interaction parameters for iPP/$C_{32}H_{66}$ system at its critical composition. Symbols as in *Figure 7*

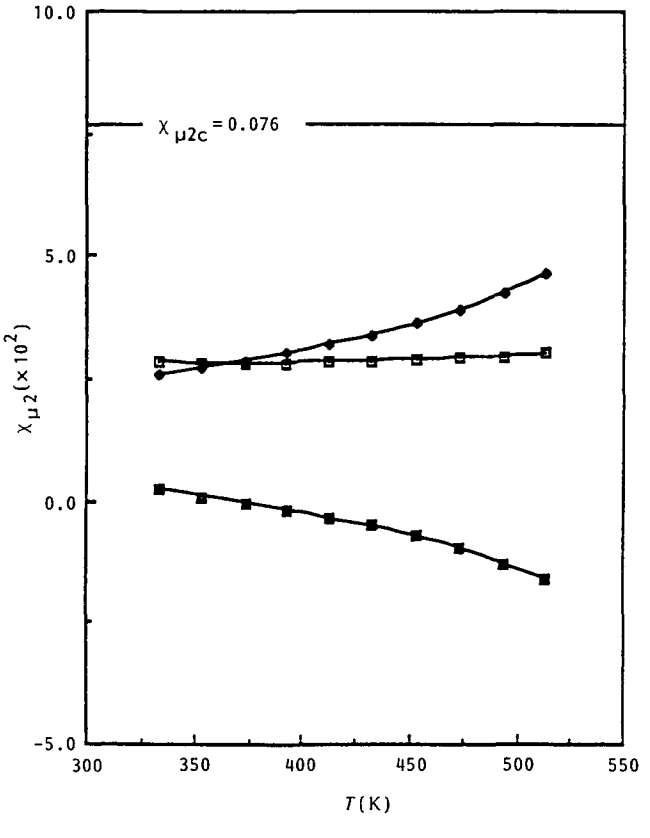

Figure 7 Contributions of enthalpic and entropic interaction parameters for iPP/$C_{20}H_{42}$ system at its critical composition: (□) $\chi_{\mu 2}$; (◆) $\chi_{\mu 2s}$; (■) $\chi_{\mu 2h}$

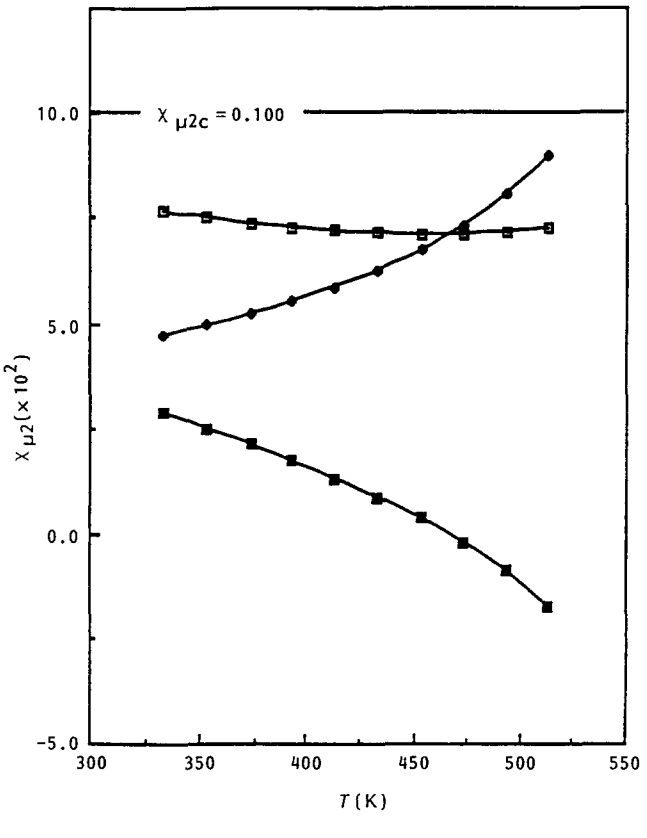

Figure 9 Contributions of enthalpic and entropic interaction parameters for iPP/$C_{14}H_{29}COOH$ system at its critical composition. Symbols as in *Figure 7*

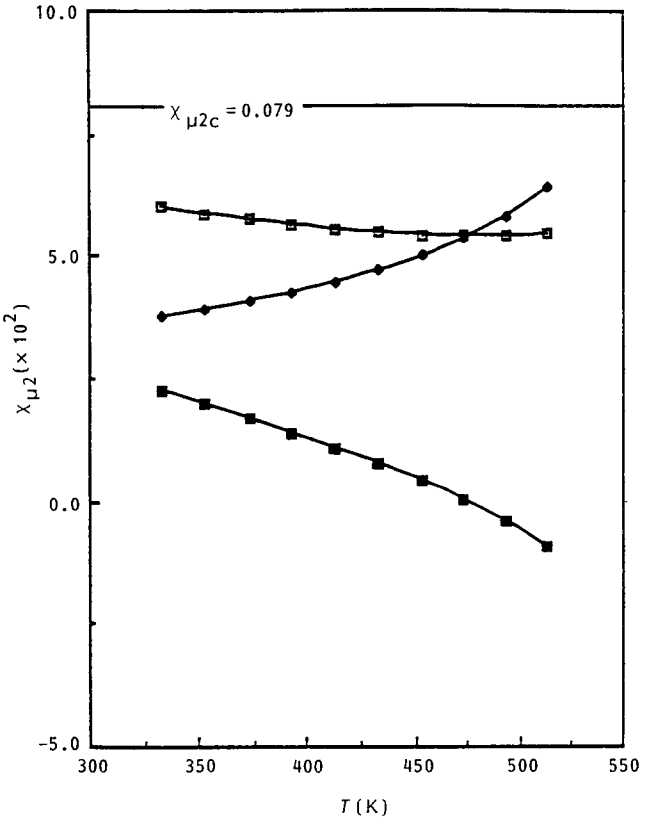

Figure 10 Contributions of enthalpic and entropic interaction parameters for iPP/$C_{19}H_{39}COOH$ system at its critical composition. Symbols as in *Figure 7*

For iPP/n-alkane systems, $\chi_{\mu 2}$ remained nearly constant with temperature change, since the changes in $\chi_{\mu 2s}$ and $\chi_{\mu 2h}$ cancelled each other. $\chi_{\mu 2}$ was smaller than $\chi_{\mu 2c}$ within the temperature range of interest shown in each plot, which means every system is stable. The *UCST* type phase separation behaviour is not expected for iPP/n-alkane systems. However, the *LCST* type phase separation is expected due to the significant free volume effect at high temperature, though it was not shown within the temperature range of each plot.

The iPP/n-fatty acid system had greater $\chi_{\mu 2}$ than the iPP/n-alkane system of equivalent chain length of diluent. $\chi_{\mu 2h}$ of the iPP/n-fatty acid system was greater than that of the iPP/n-alkane system, since the iPP/n-fatty acid system had greater enthalpic interaction (greater X_{12} parameter) than the iPP/n-alkane system. The iPP/$C_{14}H_{29}COOH$ system had greater $\chi_{\mu 2h}$ than iPP/$C_{19}H_{39}COOH$, since $C_{14}H_{29}COOH$ has a higher carboxyl group density than $C_{19}H_{39}COOH$ and thereby the iPP/$C_{14}H_{29}COOH$ system had greater enthalpic interaction (greater X_{12} parameter) than the iPP/$C_{19}H_{39}COOH$ system. The iPP/$C_{14}H_{29}COOH$ system also had greater $\chi_{\mu 2s}$ than the iPP/$C_{19}H_{39}COOH$ system, since the decrease in diluent chain length resulted in an increase in free volume effect, as discussed for iPP/n-alkane systems. Consequently, with increase of chain length of n-fatty acid, both $\chi_{\mu 2h}$ and $\chi_{\mu 2s}$ decreased, and the miscibility of the iPP/n-fatty acid system was enhanced. The ratio of $\chi_{\mu 2}/\chi_{\mu 2c}$ of iPP/$C_{19}H_{39}COOH$ was smaller than that of iPP/$C_{14}H_{29}COOH$ as listed in *Table 1*.

The change in $\chi_{\mu 2h}$ was greater than that of $\chi_{\mu 2s}$ in the temperature range of interest for iPP/n-fatty acid systems. Therefore, the $\chi_{\mu 2}$ plot decreased with increasing temperature as shown in *Figures 9* and *10*. At the lower temperature range $\chi_{\mu 2}$ is quite close to the $\chi_{\mu 2c}$ boundary, and if the temperature is lowered further it should exceed the $\chi_{\mu 2c}$ value, which means liquid–liquid phase separation will occur. If it is recalled that $\chi_{\mu 2}$ for iPP/n-fatty acid systems were underestimated in *Figure 5*, a *UCST* can be expected for iPP/n-fatty acid systems, though it is not shown in *Figures 9* and *10*.

At high temperatures $\chi_{\mu 2s}$ becomes significant, which should increase $\chi_{\mu 2}$ with increasing temperature to reach an *LCST*. Therefore, both *UCST* and *LCST* type phase separation are expected for iPP/n-fatty acid systems, though they were not shown in the temperature range of the plots.

COMPOSITION DEPENDENCE OF INTERACTION PARAMETERS

In the Flory–Huggins theory, the composition dependence of the interaction parameter is ignored. However, the composition dependence of the interaction parameter was reported in many polymer solution systems, and was predicted by EOS theory[13,24–26].

In *Figures 11* and *12*, the composition dependence of the interaction parameter near the equilibrium melting temperatures (450 K) is illustrated. For all of the iPP/n-alkane systems and the iPP/$C_{19}H_{39}COOH$ system, the interaction parameters are estimated to be nearly constant with composition, which confirms the postulation made in the $\chi_{\mu 2}$ determination from T_m depression measurements. However, there is a slight composition dependence for the iPP/$C_{14}H_{29}COOH$ system.

If the interaction parameter is composition independent, $\chi_{\mu 1}$ and $\chi_{\mu 2}$ must be identical. Therefore, the composition dependence of the interaction parameter can also be examined by comparing $\chi_{\mu 1}$ and $\chi_{\mu 2}$. $\chi_{\mu 1}$ and $\chi_{\mu 2}$ are not much different from each other for the iPP/n-alkane and iPP/$C_{19}H_{39}COOH$ systems as shown in *Figures 11*

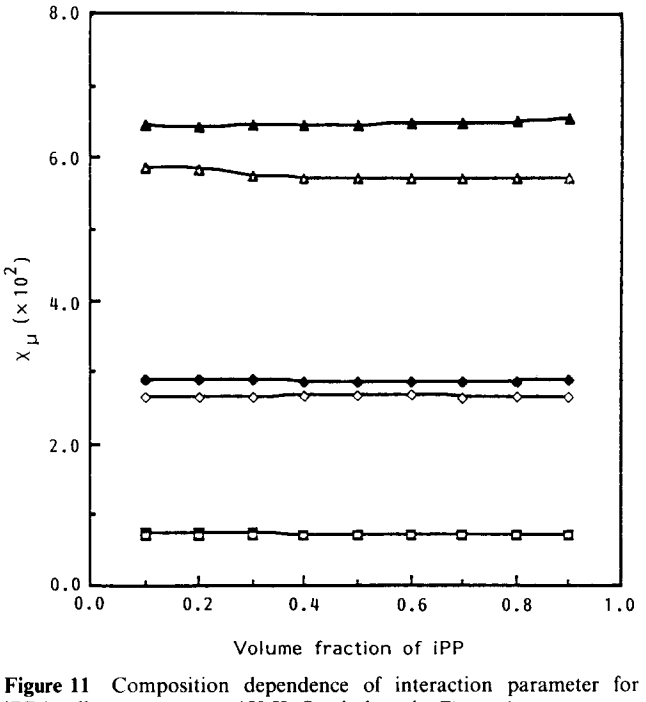

Figure 11 Composition dependence of interaction parameter for iPP/n-alkane systems at 450 K. Symbols as in *Figure 4*

and *12*, which means that the interaction parameters are not strongly composition dependent for these systems at 450 K. There is a slight deviation for the iPP/$C_{14}H_{29}$-COOH system, since there is a slight composition dependence for this system.

It was shown in *Figures 4* and *5* that the interaction parameters for the iPP/n-alkane and iPP/$C_{19}H_{39}COOH$ systems are not strongly composition dependent at temperatures other than 450 K, since $\chi_{\mu 1}$ and $\chi_{\mu 2}$ are not much different from each other. For the iPP/$C_{14}H_{29}COOH$ system, there is a slight difference between $\chi_{\mu 1}$ and $\chi_{\mu 2}$, which means that the interaction parameter was slightly composition dependent for the temperature range of interest. The difference between $\chi_{\mu 1}$ and $\chi_{\mu 2}$ was nearly independent of temperature for every system, which means the composition dependence of the interaction parameter does not change much with temperature within the temperature range of interest.

The composition dependence of the interaction parameter could have been more exactly estimated, if the EOS parameters, especially the group contribution values of surface fraction, were determined more precisely.

EQUILIBRIUM MELTING TEMPERATURE ESTIMATION

The equilibrium melting temperature of each system covered in this study was estimated using the melting temperature depression equation (equation (10), in which the interaction parameter ($\chi_{\mu 2}$) was estimated by EOS. Therefore, the equilibrium melting temperature curve, the phase boundary of solid–liquid phase separation, was estimated without any experimental work for the melting temperature depression measurement.

In *Figures 13* and *14* the estimated equilibrium melting

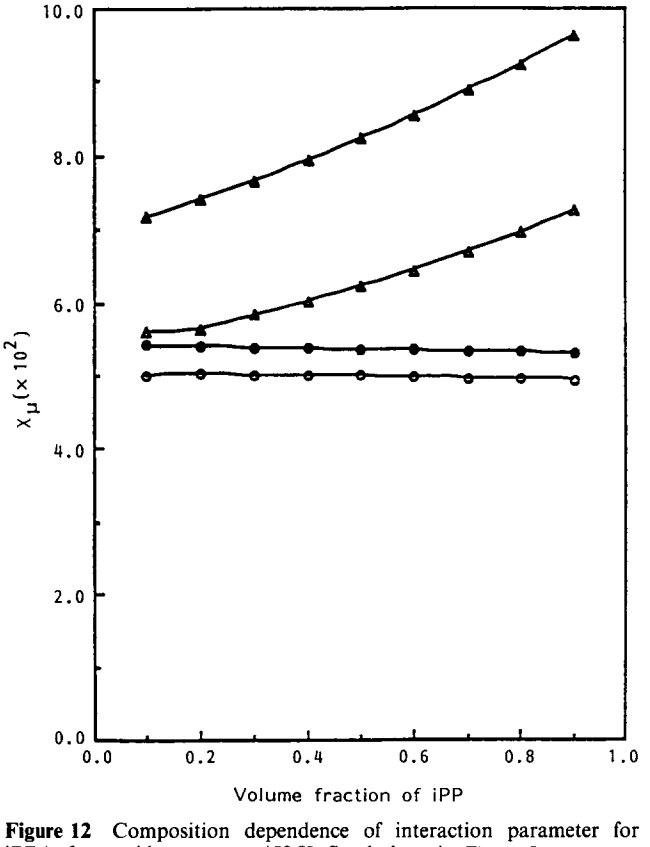

Figure 12 Composition dependence of interaction parameter for iPP/n-fatty acid systems at 450 K. Symbols as in *Figure 5*

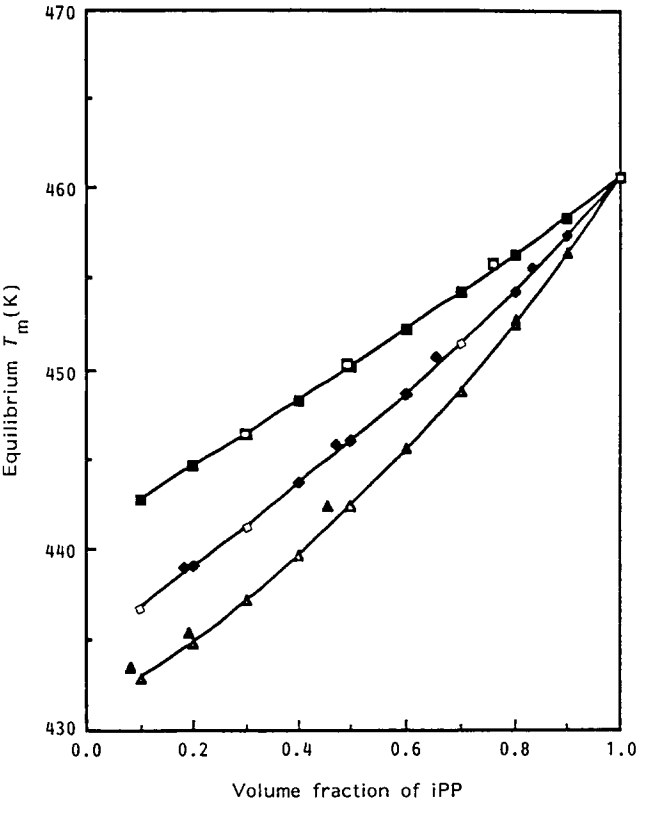

Figure 13 Comparison of experimental and estimated equilibrium melting temperature curves for iPP/n-alkane systems (open symbols: estimated; closed symbols: experimental). Symbols as in *Figure 4*

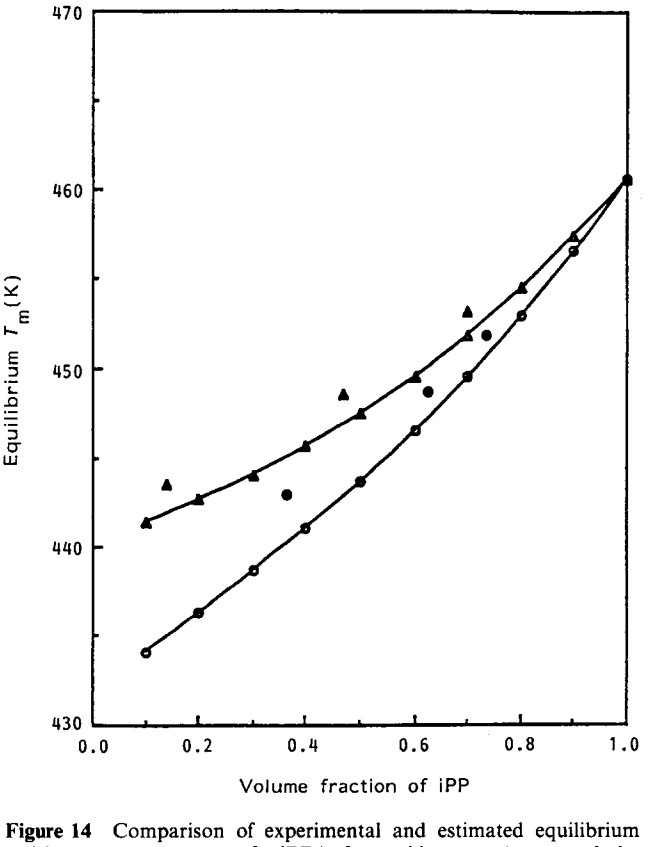

Figure 14 Comparison of experimental and estimated equilibrium melting temperature curves for iPP/n-fatty acid systems (open symbols: estimated; closed symbols: experimental): (○, ●) iPP/$C_{14}H_{29}COOH$; (△, ▲) iPP/$C_{19}H_{39}COOH$

temperatures for iPP/n-alkane and iPP/n-fatty acid systems were compared with the experimental results. For iPP/n-alkane systems, they were accurately estimated with the maximum deviation from the experimental results of <1 K. For iPP/n-fatty acid systems the estimated melting temperature depression curves were located below the experimental ones. This underestimation came from the deviation of the X_{12} parameter extrapolation for the polymeric system.

THERMODYNAMIC STABILITY OF THE SYSTEM

The thermodynamic stability conditions are[19]:

$$\Delta G/RT < 0 \tag{15}$$

$$\partial^2(\Delta G/RT)/\partial\phi_2{}^2 > 0. \tag{16}$$

For an unstable system, there are two kinds of liquid–liquid separation points: spinodal and binodal, for which there is a polymer-lean (ϕ'_2) and a polymer-rich phase (ϕ''_2). At the spinodal points (ϕ'_{2s} and at ϕ''_{2s}) equation (17) is satisfied at a certain temperature ($T = T_1$)[27].

$$[\partial^2(\Delta G/RT)/\partial\phi_2^2]_{P,T} = 0 \tag{17}$$

At the binodal points (ϕ'_{2b} and at ϕ''_{2b}) at T_1 equations (18) and (19) must be satisfied in order to draw a common tangent line[27].

$$[\partial(\Delta G/RT)/\partial\phi_2] \text{ at } \phi_{2b} = [\partial(\Delta G/RT)/\mathrm{d}\phi_2] \text{ at } \phi'_{2b} \tag{18}$$

$$\{(\Delta G/RT) - [\partial(\Delta G/RT)/\partial\phi_2]\phi_2\} \text{ at } \phi_{2b} = \{(\Delta G/RT) - [\partial(\Delta G/RT)/\partial\phi_2]\phi_2\} \text{ at } \phi'_{2b} \tag{19}$$

The details of liquid–liquid phase separation are covered in a subsequent paper in this series[27].

Since there is a significant difference in the size of iPP and diluent molecules, the number of moles of mixture is changed with the composition of the mixture. Then, these thermodynamic functions must be distorted, if they are expressed on a mole basis as shown in equation (1) in references 1 and 15. Therefore, it was more convenient to define them on the basis of the number of lattice sites. Then equations (15)–(19) must be divided by the total number of lattice sites in the system ($n_1r_1 + n_2r_2$). Then $\Delta G/RT$ must be replaced by $\Delta G^1/RT$ ($\Delta G/RT$ per lattice site).

$\Delta G^1/RT$ can be expressed in terms of EOS as the sum of the combinatorial entropy per lattice site (ΔS^{C1}), the residual entropy per lattice site (S^{R1}) and the residual enthalpy per lattice site (H^{R1}).

$$\Delta G^1/RT = (-T\Delta S^{C1} - TS^{R1} + H^{R1})/RT \tag{20}$$

where ΔS^{C1}, S^{R1} and H^{R1} are obtained by dividing ΔS^C, S^R and H^R by the total number of lattice sites which resulted in the following expressions:

$$\Delta S^{C1} = \phi_1/r_1 \ln(\phi_1) + \phi_2/r_2 \ln(\phi_2) \tag{21}$$

$$S^{R1} = -3(V_2^*/r_2)\{\phi_1(P_1^*/T_1^*)\ln[(\tilde{V}_1^{1/3} - 1)/(\tilde{V}^{1/3} - 1)] + \phi_2(P_2^*/T_2^*)\ln[(\tilde{V}_2^{1/3} - 1)/(\tilde{V}^{1/3} - 1)]\} \tag{22}$$

$$H^{R1} = (V_2^*/r_2)\{\phi_1 P_1^*(\tilde{V}_1^{-1} - \tilde{V}^{-1}) + \phi_2 P_2^*(\tilde{V}_2^{-1} - \tilde{V}^{-1}) + [(\phi_1\theta_2)(X_{12}/\tilde{V})]\} \tag{23}$$

$\partial(\Delta G^1/RT)/\partial\phi_2$ was obtained by differentiating equations (20)–(23), and was simplified by using $\chi_{\mu 2}$ as introduced in equation (7).

$$\partial(\Delta G^1/RT)/\partial\phi_2 = -\ln(\phi_1)/r_1 + \ln(\phi_2)/r_2 + (1/r_2 - 1/r_1) + \chi_{\mu 2}(\phi_1 - \phi_2) \tag{24}$$

The second derivative of $\Delta G^1/RT$ was obtained by differentiating equation (24), where the composition dependence of $\chi_{\mu 2}$ was considered.

$$\partial^2(\Delta G^1/RT)/\partial\phi_2^2 = 1/(r_1\phi_1) + 1/(r_2\phi_2) - 2\chi_{\mu 2} + (\phi_1 - \phi_2)\,\partial\chi_{\mu 2}/\partial\phi_2 \tag{25}$$

where $\partial\chi_{\mu 2}/\partial\phi_2$ can be obtained from equation (1) as

$$\partial\chi_{\mu 2}/\partial\phi_2 = \{[\partial(\Delta\mu_2^R/RT)/\partial\phi_2] + 2r_2\phi_1\chi_{\mu 2}]\}/r_2\phi_1^2 \tag{26}$$

A derivative of the residual chemical potential in terms of ϕ_2 was obtained as

$$\begin{aligned}\partial(\Delta\mu_2^R/RT)/\partial\phi_2 &= (P_2^*V_2^*/RT_2^*)[-(\partial\tilde{V}/\partial\phi_2)/(\tilde{V} - \tilde{V}^{2/3})] \\ &\quad + [P_2^*V_2^*(\partial\tilde{V}/\partial\phi_2)/RT\tilde{V}^2] \\ &\quad - [(2V_2^*/RT)(X_{12}/\tilde{V})(\theta_2/\phi_2)^3\phi_1] \\ &\quad - [V_2^*X_{12}(\partial\tilde{V}/\partial\phi_2)(\theta_2^2/RT\tilde{V}^2)(\phi_1/\phi_2)^2]\end{aligned} \tag{27}$$

The derivatives of reduced parameters were obtained according to Sham and Walsh's method[17,28].

$$(\partial\tilde{V}/\partial\phi_2) = \{\partial\tilde{P}/\partial\phi_2 - [(\tilde{P} + 1/\tilde{V}^2)/\tilde{T}](\partial\tilde{T}/\partial\phi_2)\} /\{(2/\tilde{V}^3) - [\tilde{T}(\tilde{V}^{1/3} - 2/3)] /[\tilde{V}^{5/3}(\tilde{V}^{1/3} - 1)^2]\} \tag{28}$$

$$(\partial\tilde{P}/\partial\phi_2) = P/P^{*2}\{P_1^* - P_2^* - X_{12}\theta_2[1 - (\theta_1/\phi_2)]\} \tag{29}$$

$$(\partial\tilde{T}/\partial\phi_2) = [\tilde{T}(\partial\tilde{P}/\partial\phi_2)/\tilde{P}] + [(P_2^*\tilde{T}_2 - P_1^*\tilde{T}_1)/P^*] \tag{30}$$

$\Delta G^1/RT$, $\partial(\Delta G^1/RT)/\partial\phi_2$ and $\partial^2(\Delta G^1/RT)/\partial\phi_2^2$ were estimated by the above equations for various compositions and temperatures. The plots of the iPP/$C_{20}H_{42}$ and iPP/$C_{19}H_{39}$COOH systems are shown in *Figures 15–20*. The plots of the iPP/$C_{14}H_{30}$ and iPP/$C_{32}H_{66}$ systems have similar trends to those of the iPP/$C_{20}H_{42}$ system, and are shown in reference 23. The plots of the iPP/$C_{14}H_{29}$COOH system are similar to the iPP/$C_{19}H_{39}$COOH system, and are also shown in reference 23.

As shown in *Figures 15* and *16*, $\Delta G^1/RT$ is always negative for the iPP/$C_{20}H_{42}$ and iPP/$C_{19}H_{39}$COOH systems within the temperature range of interest, and this was true for the other n-alkane or n-fatty acid systems. $\Delta G^1/RT$ of the iPP/$C_{20}H_{42}$ system was smaller than that of the iPP/$C_{19}H_{39}$COOH system; therefore, the iPP/n-alkane system is more miscible than the equivalent iPP/n-fatty acid system with similar diluent chain length. The first stability conditions as shown in equation (15) were satisfied for iPP/n-alkane and iPP/n-fatty acid systems.

In *Figures 17* and *18* the plots of $\partial(\Delta G^1/RT)/\partial\phi_2$ *versus* ϕ_2 are shown for iPP/$C_{20}H_{42}$ and iPP/$C_{19}H_{39}$COOH systems within the temperature range of interest. Since each $\partial(\Delta G^1/RT)/\partial\phi_2$ plot is monotonically increasing with increasing ϕ_2 within the temperature range of interest, the binodal point conditions of equations (18) and (19) are not satisfied. This is also true for the other

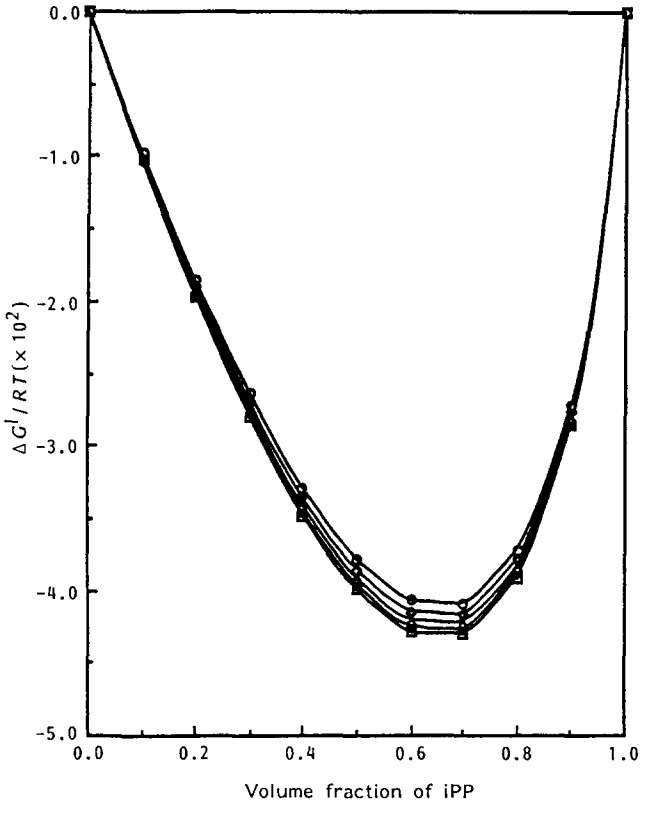

Figure 15 $\Delta G/RT$ per lattice site for iPP/$C_{20}H_{42}$ system: (□) 333 K; (◆) 373 K; (▲) 413 K; (◇) 453 K; (○) 493 K

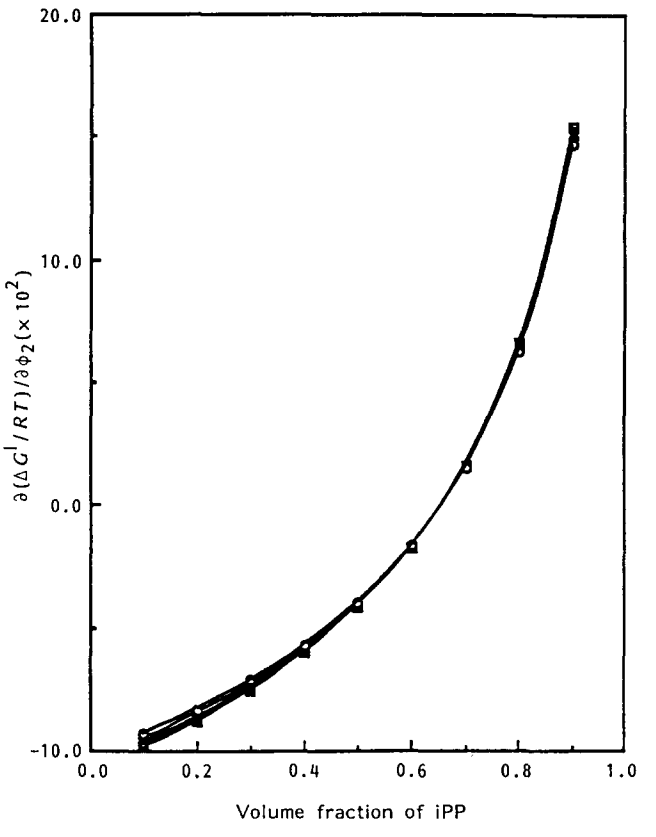

Figure 17 First derivative of $\Delta G/RT$ per lattice site for iPP/$C_{20}H_{42}$ system. Symbols as in *Figure 15*

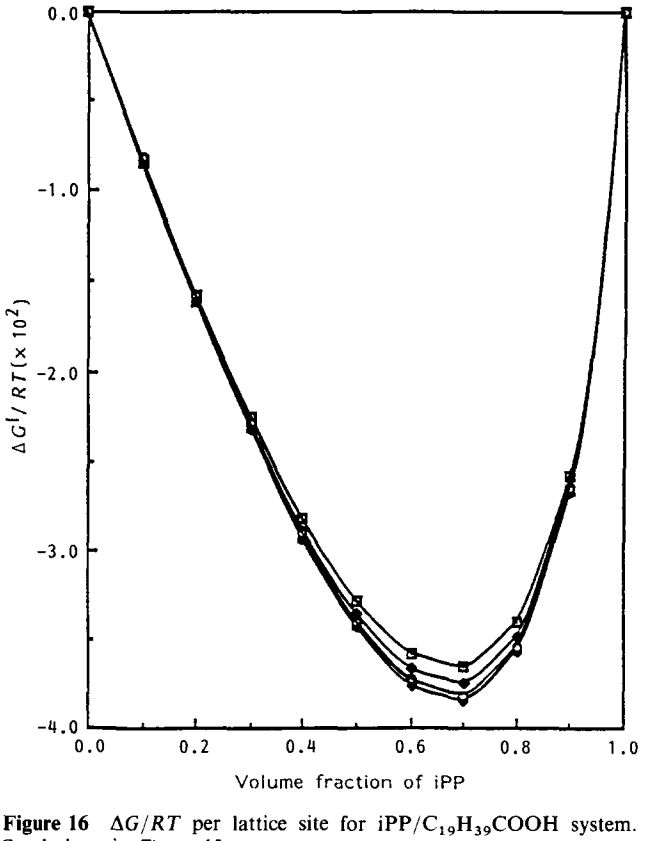

Figure 16 $\Delta G/RT$ per lattice site for iPP/$C_{19}H_{39}COOH$ system. Symbols as in *Figure 15*

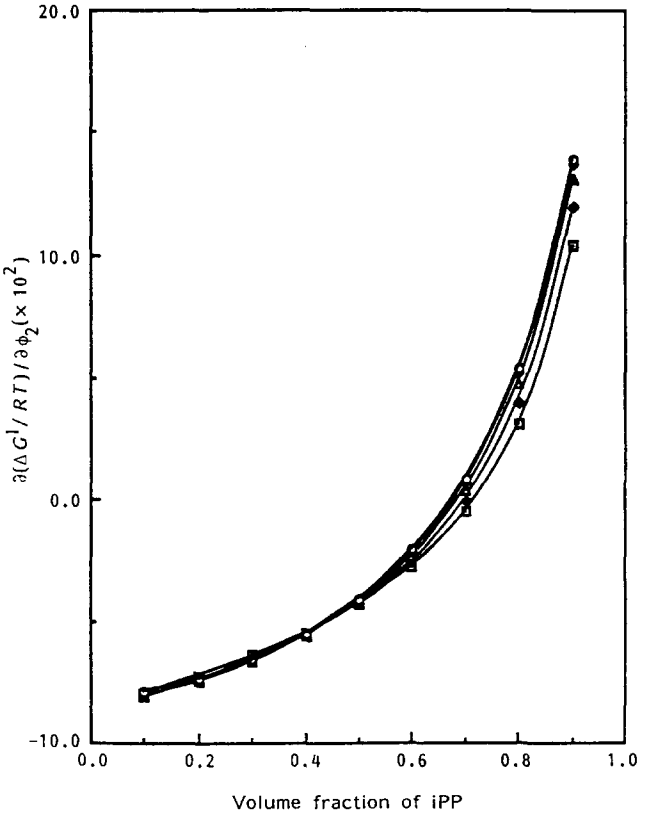

Figure 18 First derivative of $\Delta G/RT$ per lattice site for iPP/$C_{19}H_{39}COOH$ system. Symbols as in *Figure 15*

systems, the plots of which are shown in reference 23. However, the iPP/n-fatty acid system might have satisfied the binodal conditions at low temperatures if the X_{12} parameter had been more accurately determined.

In *Figures 19* and *20* $\partial^2(\Delta G^1/RT)/\partial\phi_2{}^2$ was shown within the temperature range of interest for the iPP/$C_{20}H_{42}$ and iPP/$C_{19}H_{39}COOH$ systems. Every point is positive and satisfies the second stability condition as shown in equation (16). This is also true for the other systems, and spinodal points are not expected. If the X_{12} parameter was more accurately determined for iPP/n-fatty acid systems, there may be some negative points at low temperature, where the system was unstable.

CONCLUSIONS

The interaction parameters and the phase diagrams of iPP/n-alkane and iPP/n-fatty acid systems, estimated by Flory's EOS theory were in good agreement with the experimental data from equilibrium melting temperature measurements. The free volume effect was significant for these polymer/diluent systems, which illustrated the advantage of the EOS theory over the Flory–Huggins theory. This study allows the tracing of the variation of the interaction parameter with temperature and composition change during TIPS.

Simplified methods of determining the EOS parameters, as introduced in reference 1, proved to be reliable. For iPP/n-alkane systems the free volume effect was dominant, and the interaction parameter was nearly independent of temperature due to the mutual cancellation of the changes in enthalpic and entropic interaction parameters. The interaction parameter decreased with increasing n-alkane chain length due to decreasing free volume effect. The iPP/n-fatty acid systems have greater interaction parameters than those of iPP/n-alkane systems. The iPP/n-fatty acid systems have greater enthalpic interactions than the iPP/n-alkane systems due to the carboxyl group at the end of the chain. The interaction parameters of the iPP/n-fatty acid systems decreased with increasing temperature due to the dominating enthalpic interaction. With increasing n-fatty acid chain length, the interaction parameter decreased, since both enthalpic and entropic interaction decreased.

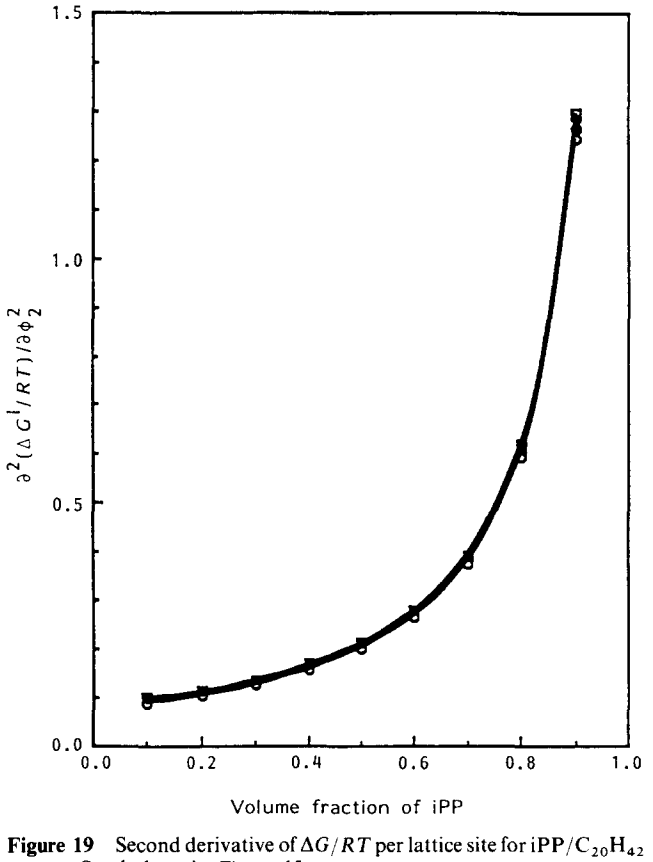

Figure 19 Second derivative of $\Delta G/RT$ per lattice site for iPP/$C_{20}H_{42}$ system. Symbols as in *Figure 15*

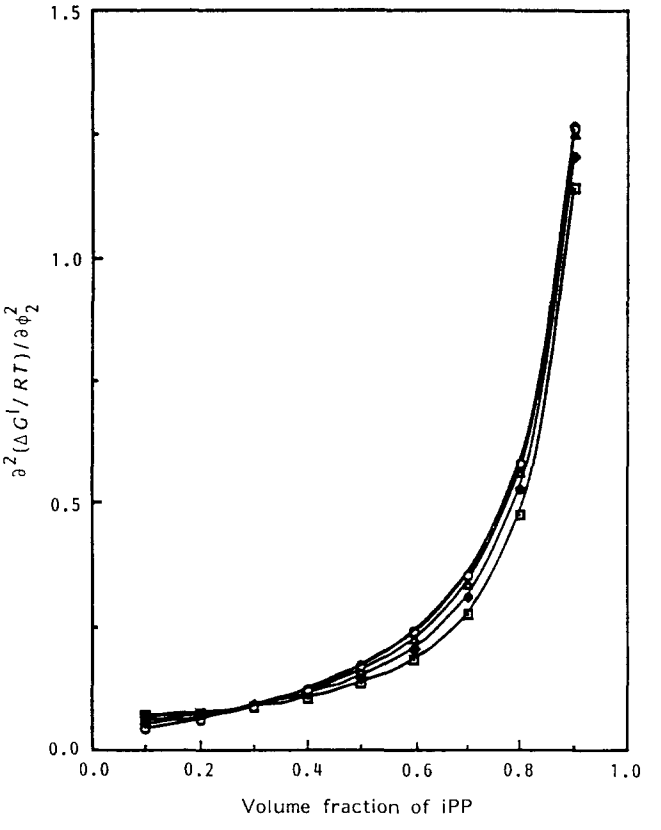

Figure 20 Second derivative of $\Delta G/RT$ per lattice site for iPP/$C_{19}H_{39}COOH$ system. Symbols as in *Figure 15*

It was confirmed that iPP/n-alkane systems were stable within the temperature range of interest. Therefore, liquid–liquid phase separation is not expected and solid–liquid phase separation via iPP crystallization is the only phase separation mechanism possible for these systems. iPP/n-fatty acid systems were also estimated to be stable within the temperature range of interest. However, they are expected to be unstable at temperatures below the iPP crystallization curves. This instability would be predictable if the X_{12} parameters were more accurately extrapolated.

ACKNOWLEDGEMENTS

The authors gratefully acknowledge the continued generous financial support of the Central Research Technology Development Laboratory of the 3M Company, St Paul, MN and Texas Advanced Technology Program.

REFERENCES

1 Kim, S. S. and Lloyd, D. R. *Polymer* 1992, **33**, 1026
2 Lloyd, D. R., Kinzer, K. E. and Tseng, H. S. *J. Membr. Sci.* 1990, **52**, 239
3 Lloyd, D. R., Kim, S. S. and Kinzer, K. E. *J. Membr. Sci.* 1991, **64**, 1

4 Kim, S. S. and Lloyd, D. R. *J. Membr. Sci.* 1991, **64**, 13
5 Lim, G. B. A., Kim, S. S., Ye, Q. H., Wang, Y. F. and Lloyd, D. R. *J. Membr. Sci.* 1991, **64**, 31
6 Kim, S. S., Lim, G. B. A., Alwattari, A. A., Wang, Y. F. and Lloyd, D. R. *J. Membr. Sci.* 1991, **64**, 41
7 Alwattari, A. A. and Lloyd, D. R. *J. Membr. Sci.* 1991, **64**, 55
8 Lloyd, D. R., Barlow, J. W. and Kinzer, K. E. *AIChE Symp. Ser. 261* 1989, **84**, 28
9 Smolders, C. A., van Aartsen, J. J. and Steenbergen, A. *Kolloid-Z. Z. Polym.* 1971, **243**, 14
10 Castro, A. J. *US Pat. 4 247 498*, 1981
11 Flory, P. J., Orowoll, R. A. and Vrij, A. *J. Am. Chem. Soc.* 1964, **86**, 3507
12 Eichinger, B. E. and Flory, P. J. *Trans. Faraday Soc.* 1968, **64**, 2035, 2053, 2961, 2066
13 Flory, P. J. *Discuss. Faraday Soc.* 1970, **49**, 7
14 Sanchez, I. C. *Polymer* 1989, **30**, 471
15 Sanchez, I. C. *Macromolecules* 1978, **11**, 1145
16 Chahal, R. S., Kao, W.-P. and Patterson, D. *Faraday Trans. I.* 1973, **69**, 1834
17 Sham, C. K. and Walsh, D. J. *Polymer* 1987, **28**, 804
18 Nishi, T. and Wang, T. T. *Macromolecules* 1975, **18**, 909
19 Flory, P. J. 'Principles of Polymer Chemistry', Cornell University Press, Ithaca, 1965, pp. 507–576
20 Wunderlich, B. 'Macromolecular Physics, Vol. III, Crystal Melting', Academic Press, New York, 1980, pp. 61–64
21 Lim, G. B. A. *PhD Dissertation* The University of Texas at Austin, 1990
22 Hoffman, J. D. and Weeks, J. J. *J. Res. Natl Bur. Stand.* 1962, **66**, 13
23 Kim, S. S. *PhD Dissertation* The University of Texas at Austin, 1990
24 Han, C. C., Bauer, B. J., Clark, J. C., Muroga, Y., Matsushita, Y., Okada, M., Tran-cong, Q., Chang, T. and Sanchez, I. C. *Polymer* 1988, **29**, 2002
25 Sanchez, I. C. and Balazs, A. C. *Macromolecules* 1989, **22**, 2325
26 Sanchez, I. C. in 'Encyclopedia of Physical Science and Technology', Vol. XI, Academic Press, New York, 1987, pp. 1–18
27 Kim, S. S. and Lloyd, D. R. *Polymer* 1992, **33**, 1047
28 Rostami, S. and Walsh, D. J. *Macromolecules* 1984, **17**, 315